and FIN STABILIZER EFFECT

Rahimuddin, Adi Maimun Abdul Malik, Muhamad Pauzi Abdul Ghani
Universiti Teknologi Malaysia, Johor Malaysia
rahimnav@gmail.com

ABSTRACT

A Semi-SWATH ship is a high ship speed build as a hybrid design of catamaran and SWATH (Small Waterplane Area Twin Hull) design. The ship has a lack of tending to a bow-dive condition when running in wave high in following sea. The slender and low buoyancy force at the bow hull causes the tendency of the condition is increase. A parametric study developed to investigate the lack and increase the ship behavior using fixed and active fin stabilizer. A numerical simulation developed for 3DoF (surge, heave, and pitch) based on strip theory, and validated using seakeeping test in towing tank. The simulation found the ship with fixed fin at bow and active fin at stern has a better performance, prevent the bow-dive condition and then reduced the possibility of immersed foredeck. However, the tendency of immersed foredeck in longer wavelength is increase, whilst the ship with all fixed fin stabilizer is decrease.

Keywords; bow-dive, semi-SWATH

INTRODUCTION

The excellence of multihull ship in seakeeping affects the demand of the ship increased. In 2005, Papanikolaou has presented a systematically data for a high-speed ship type and advance marine vehicle type in worldwide. He recorded catamaran has been used widely in the world was 34.1% whilst SWATH 1.2% and semi-SWATH 1.4% of 653 ships recorded throughout the world. The famous aspect of catamaran was the high speed with low cost of ship structure and ship maintenance than SWATH ship. He estimated that demand of the semi-SWATH would increase along with the advances in the technology and design of the ship, (Papanikolaou & Soares, 2009).

Currently, demand of the high-speed ship is developing, and it not only increases the ship dimension but also the ship performances in bad weather condition. It was particularly the ship with a good comfort in service and safety in navigation, (Folso, 2004; Stevens & Parsons, 2002). To address the purpose of the high-speed ship cannot ignore the occurrence of the dynamic motion caused by the hydrodynamic forces acting on the hull of ship. It is considerably different to conventional monohull ship where the ship has low speed and risk in the ship navigation.

Regarding to the dynamic of the ship in following seas, in 2006, Dand has investigated the dynamic motion of Catamaran in towing tank. He found the ship tends to have a surfing condition when amidships has just been passing the crest, (Dand, 2006). The ship experienced the condition, increased speed that accelerated by the effect of weight force during the ship in wave-down. As well as the low restoring force at fore hull affect the ship experience a bow-dive condition (Fang & Chan, 2004). The rapidly acceleration of the ship in wave-down indicated the ship experienced a surfing condition (Matsuda, Hasimoto, & Umeda, 2004)

Design of the semi-SWATH with fin stabilizer at fore and aft ends of hulls used to decrease the effect of porpoising. The effect was increased by the increased of the ship's speed in head seas. Moreover, in following seas, the fin may decrease the effect of having a surf-riding and bow-diving effect. The fins act as a wing-foil aim to increase the lift force and damping force.

Over thirty-five years past, the fin applications mostly were to maintain the roll motion of monohull ship. However, along with an increase of the ship's speed, the dynamic of vertical motion increased. Semi-SWATH ship is one that indicated has a dynamic vertical motion with the increase of speed even porpoising phenomenon occurs as a drawback of the ship. Application of the fin stabilizer in a proper manner might increase the ship damping to restrain the effect of external forces and moment, (Bhattacharya, 1978; Djackov, 2005).

In this paper, the dynamic motion of the semi-SWATH in following seas and the effects of the fin stabilizer were studied using time domain simulation.

MATHEMATICAL MODEL

SHIP MOTION MODEL

The mathematical model of the ship motion was modeled in 3DoF consists of surge, heave, and pitch motion. The ship motion can be expressed in the coordinate system of translational and rotational motion, using the right hand rules. Ship movements generally translated in two coordinates of space systems. One reference is fixed coordinate system on earth (OXYZ) and another one is moving coordinate system located on the ship (OXsYsZs). The fixed coordinate system located at a calm water surface with Z-axis pointing upwards. Moving coordinate system is located at the centre of gravity, moving with speed Vs, as shown in Figure 1 and Figure 2.

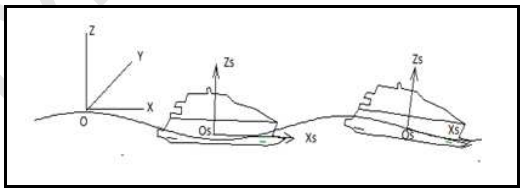

Figure 1 Fixed and moving coordinate axis.

The harmonic motions of the ship in longitudinal and vertical motions were considered. Coupling effect between both motions is negligible. It can be ignored in simulation (Umeda, 1990), whilst the coupling effect between the heave and pitch is significant (Lloyd, 1998).

The motions were expressed in second order of linear differential equations, *m* is mass, *a* is added mass, *b* is damping and *c* is restoring coefficients. Index *1,3,5* indicate surge, heave and pitch respectively and F is force or moment of wave as in following form;

$$(a_{11}+m)\ddot{x}_1+[R(u)-T(u,n)]=F_1^W-mg\sin\theta \quad (1)$$

$$(a_{33}+m)\ddot{x}_3+b_{33}\dot{x}_3+c_{33}x_3+a_{35}\ddot{x}_5+b_{35}\dot{x}_5+c_{33}x_5=F_3+mg\cos\theta \quad (2)$$

$$a_{53}\ddot{x}_3+b_{53}\dot{x}_3+c_{53}x_3+(a_{55}+I_{55})\ddot{x}_5+b_{55}\dot{x}_5+c_{55}x_5=F_5-x_Smg\cos\theta \quad (3)$$

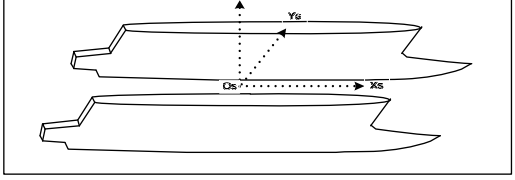

Figure 2 The origin of coordinate axis of a multihull ship at centre of gravity.

Surge motion is a longitudinal motion that superimposed on propeller thrust, hull resistance, and incident wave of Froude-Krylov harmonic force, (Spyrou & Tingkas, 2011; Umeda, 1990; Wu, Spyrou, & McCue, 2010). In this paper, the vertical motion of heave and pitch influenced by the effect of ship weight in wave slope in which the surge motion is changed in harmonic. The changes affect encounter frequency changed, and hydrodynamic coefficients should be updated. The model was integrated with fin stabilizer into the equations (1) as follows;

$$\begin{aligned}&(a_{11}+m)\ddot{x}_1+\left\{[3r_3c^2+2(r_2-\tau_2)c+r_1]-\tau_1 n\right\}\dot{x}_1\cdots\\&+\left[3r_3c+(r_2-\tau_2)\right]\dot{x}_1^{\,2}+r_3\dot{x}_1^{\,3}=(\tau_2c^2+\tau_1cn+\tau_0n^2)\cdots\\&-(r_1c+r_2c^2+r_3c^3)-f\sin(kx_1)-mg\sin x_5+F_1^{\,f}\end{aligned} \tag{4}$$

$$\begin{aligned}&(a_{33}+m+a_{33}^{f}+m_f)\ddot{x}_3+(b_{33}+b_f)\dot{x}_3+c_{33}x_3\cdots\\&+(a_{35}-l(m_f+a_{33}^{f})\ddot{x}_5+(b_{35}-b_f)\dot{x}_5+(c_{35}+c_{35}^{f})x_5\cdots\\&=F_3^{w}+F_3^{f}+mg\cos x_5\end{aligned} \tag{5}$$

$$\begin{aligned}&(a_{53}-l(m_f+a_{33}^{f})\ddot{x}_3+(b_{53}-b_f)\dot{x}_3+c_{53}x_3+(a_{55}+I_{55}\cdots\\&+l^2(m_f+a_{33}^{f}))\ddot{x}_5+(b_{55}+b_f)\dot{x}_5+(c_{55}-c_{55}^{f})x_5\cdots\\&=F_5^{w}+F_5^{f}-x_{S(G)}mg\cos x_5\end{aligned} \tag{6}$$

Since x is the surge displacement from a wave crest, $\dot{x}$ is a relative velocity of ship to the wave celerity, $\dot{x}=u-c$ where u and c are the ship speed and wave celerity. Superscript of w, f indicate wave, fin respectively. Coefficients r, and τ were the polynomial coefficients determined in thrust empirical calculation and resistance test.

The hydrodynamic coefficients of the ship motion determined by a mixed of numerical and experiment task. The hydrodynamic coefficients of heave and pitch motion determined using Frank Close fit method while the surge motion coefficients determined from surge force oscillation test, resistance test, and empirical equation of propeller thrust.

FIN STABILIZER MODEL

The mathematical model of a servo control of the fin stabilizer is based on first-order equation in Laplace's function, (Amerongen, 1982; Klught, 1987). The model of the steering rudder machine with settling time τ_r, desired fin angle δ_d, and fin angle δ as well, written as follows;

$$\frac{\delta(s)}{\delta_d(s)}=\frac{1}{1+\tau_r s} \tag{7}$$

in the form of inverse Laplace form written as follows;

$$\delta(t)=\int_0^{\infty}e^{-\tau_r t}e^{-st}\delta_d(t)dt \tag{8}$$

The exciting force and moments obtained from the integration of incident wave pressure up to the free surface (Bhattacharya, 1978; Chin, Roberts, Scrace, & Owens, 1994; Faltinsen, 2005; Maimun, 1993), where the wave profile offset obtained as follows;

$$\zeta(t)=\zeta_a\frac{\sinh k(-z+h)}{\sinh kh}\cos k(x-V_w t) \tag{10}$$

The water surface profile defined at surface, $z=0$ as follows;

$$\zeta=\zeta_a\cos k(x-V_w t) \tag{11}$$

and the regular wave celerity obtained as follows;

$$V_w=\sqrt{\frac{g\,L_w}{2\,\pi}} \tag{12}$$

The water celerity in horizontal (u) and vertical (w) orbital obtained as follows;

$$u=k\zeta_a V_w e^{-kz}\cos k(x-V_w t) \tag{13}$$

$$w=k\zeta_a V_w e^{-kz}\sin k(x-V_w t) \tag{14}$$

The wave profile is assumed the presence of the ship does not result in any pressure disturbance. Then, force and moment were obtained as follows;

$$F_w=-\iiint_V p\,dV \qquad M_w=-\iiint_V p\,r\,dV \tag{15}$$

The surrounding fluid is assumed ideal, irrotational, incompressible and in viscid. The pressure p acts on the surface element at r vector position from CG. The pressure can be described by the Bernoulli's equation in the following way;

$$p=-\rho qz-\rho\frac{\partial\Phi}{\partial t}-\frac{1}{2}\rho(grad\,\Phi)^2 \tag{16}$$

From the total velocity potential Φ, where;

$$\Phi=-Ux+\phi_S+\phi_I e^{i\omega t} \tag{17}$$

The last term in the time dependent velocity potential associated with unsteady body motion, incident and diffracted waves. By assume that the presence of the ship does not cause any distortion to the waves, the forces due to the diffracted potential can be neglected and the excitation force derived from the incident waves, which termed by the Froude Krylov force and moments.

The vertical force and moment acting overall on the ship was obtained by integration of force and moment of sections, (Maimun, 1993). The integration equation derived as follows;

$$F_1^{w}=-\rho g\zeta k\int_{-L/2}^{+L/2}e^{-kd(x)}S(x)\sin k(x_0+x_s-ct)dx \tag{18}$$

$$F_3^{w}=-\rho g\cos\theta\int_{-L/2}^{+L/2}S(x,t)\,dx-\rho g\zeta k\int_{-L/2}^{+L/2}e^{-kd(x,t)}S(x,t)\cos k(x-ct)dx \tag{19}$$

$$F_5^{w}=\rho g\cos\theta\int_{-L/2}^{+L/2}x_S S(x,t)\,dx+\rho g\zeta k\int_{-L/2}^{+L/2}e^{-kd(x,t)}S(x,t)\cos k(x-ct)dx \tag{20}$$

Where, *S(x,t)* is the unit ship surface at *x* position and at *t* time with *c* is a relative speed of ship and wave.

PROPELLER THRUST FORCE AND RESISTANCE

The thrust of a ship propeller depends on the volume of water accelerated per time unit, on the amount of the acceleration, and on the density of the medium. Conventionally, the ship propeller characterized in open-water propeller is presented in the form of the

propeller revolution. The coefficient can be expressed in polynomial equation of J using the graph of Wageningen B-Series propeller, where Dp, is propeller diameter, and np is a number of propeller revolution.

In the sea wave, the dynamic of submerged of propellers influenced by the ship motion interaction to the wave. It caused there a perturbation of water velocity incoming propeller. The velocity perturbation calculated as the mean of water velocity along the propeller diameter, (Spyrou & Tingkas, 2011). Then, the water velocity of incoming propeller calculated as follows;

$$u \approx u_0 + u_{(p)} \tag{21}$$

$$u \approx u_0 + \frac{1}{D_p}\int_{D_p} k\zeta_a V_w e^{-kz}\cos k(x - V_w t)dz \tag{22}$$

$$\begin{aligned} T(u,n) &= (1-t_p)\rho n^2 D_P^4 K_T(u;n) \\ K_T(u;n) &= K_0 + K_1 J(u;n) + K_2 J^2(u;n) \\ J(u;n) &= \frac{V_A}{nD_P} \end{aligned} \tag{23}$$

$$\begin{aligned} T(u;n) &= \tau_0 n^2 + \tau_1 un + \tau_2 u^2 \\ \tau_0 &= \kappa_0(1-t_P)\rho D_P^4 \\ \tau_1 &= \kappa_1(1-t_P)(1-w_P)\rho D_P^3 \\ \tau_2 &= \kappa_2(1-t_P)(1-w_P)^2\rho D_P^2 \end{aligned} \tag{24}$$

The advance speed of water determined from the known propeller wake fraction. The wake fraction caused by the presence of the hull and the free surface, is a simple measure of the change in propulsion inflow as compared to an equivalent open-water. The wake of the ship propulsion determined equal to the wake coefficient of combatant high-speed ship usually in range from 0.01 to 0.04, (Kim, 1992). The advance speed (V_A) obtained as follows;

$$V_A = u(1-w_P) \tag{25}$$

The thrust parameter of the surge motion equation was developed as a function of ship speed and propeller revolution (Spyrou, 2006; Spyrou & Tingkas, 2011). The resistance aspect in the longitudinal motion determined from the test in towing tank. The result of the resistance test developed in polynomial equation as function of ship speed u=Vs as follows;

$$R(u) = r_1 u + r_2 u^2 + r_3 u^3 \tag{26}$$

Added mass of the ship with fins stabilizer for the surge equation can be obtained from the oscillation test, (Brien & Kuchenreuther, 1957). The resistance parameter of the surge motion equation derived from the resistance test in calm water, represented in a polynomial form function of ship speed (u).

FIN FORCE AND MOMENT

The force and moment of fin stabilizer calculation using the wing model equation, influenced by the angle of attack and the losses of effective lift of fin (E). The losses of lift of fin consist of; losses by the submergence of fin, interaction of fore and aft fin and hull boundary layer. The losses of lift coefficient is obtained using empirical data of a fin combination that found in research of Lloyd, (Kenevissi, Atlar, & Mesbahi, 2003; Lloyd, 1998).

$$E = \frac{Efective\ lift\ of\ \ fin}{Nominal\ lift\ of\ \ fin}$$

The lift force and moment of fins along the projected fin area A were obtained as follows;

$$\begin{aligned} F_D &= \tfrac{1}{2}\rho V_S^2\, A\, E\, C_D(\alpha) \\ M &= F_L\, l_f \end{aligned} \tag{27}$$

Total fin angle α_f to the normal axis of motion consist of pitch angleθ, fin angle δ, and attack angle α by incoming flow to axis of fin as shown in Figure 3. The ship speed V_s = u and the vertical water velocity, υ.

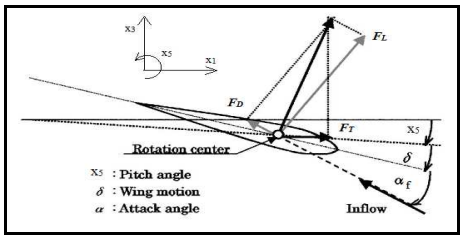

Figure 3 Vector force of fin stabilizer

The fin stabilizer has a symmetrically streamlined section. At a small angle of attack, the lift coefficient $(dC_L/d\alpha)$ increases linearly with the incidence angle. The lift curve slope of rectangular plan forms as a function of an aspect ratio written as follows,(Whicker & Fehlner, 1958);

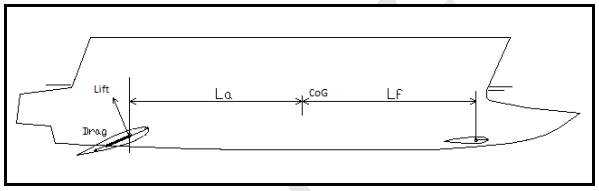

Figure 4 Longitudinal position of fin stabilizer

$$\frac{dC_L}{d\alpha} = \frac{1.8\,\pi\, a_F}{1.8 + \sqrt{a_F^2 + 4}} \quad rad^{-1} \tag{28}$$

Lift and drag coefficients CL and CD were calculated as follows;

$$C_L(\alpha) = \frac{dC_L}{d\alpha}\,\alpha \qquad C_D(\alpha) = C_{D0} + \frac{C_L^2(\alpha)}{0.9\,\pi\, a} \tag{29}$$

CD0 is the minimum section drag. In this research the minimum section drag coefficient is CD0=0.0065, (Perez, 2005).

VALIDATION OF MATHEMATICAL MODEL

FIN STABILIZER

The response of the fin stabilizer system is validated by comparing the response of the fin servo control system. Pulse signal used to trigger the fin servo system and the response compared to the simulation model of fin stabilizer as shown in Figure 5.

SHIP MOTION

The seakeeping test use captive model to validate the ship motions. The test restrains the surge motion and measure the longitudinal force of the model from wave trough to wave crest and vice versa. as shown in Figure 7,. Ratio of the model speed to wave celerity was set to 1.13, the wave steepness was 0.06 and the wave length to ship length ratio was 1.0. The model attached to air strut of the carriage and running in constant speed as shown in Figure 6.

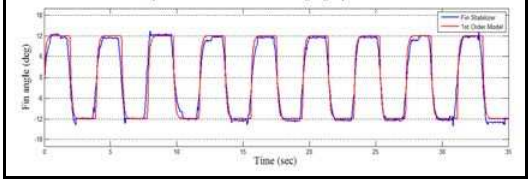

Figure 5 Response of servo control system of motor (exp) and first order of servo model (sim), τr=0.6 sec.

SURGE MOTION

Validation of surge motion is obtained by comparing the simulation results of surge force and the force measured in the test when the model is advancing the waves Figure **6**. This is regarding to the Newton's 2nd Law of motion that the relationship between the longitudinal acceleration of the ship is linear to the force acting on it.

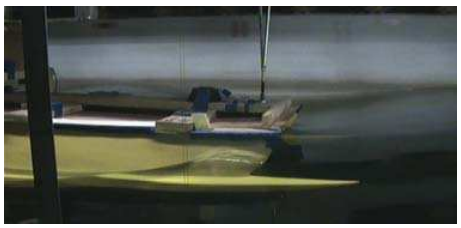

Figure **6** Seakeeping test in following sea, conducted in towing tank

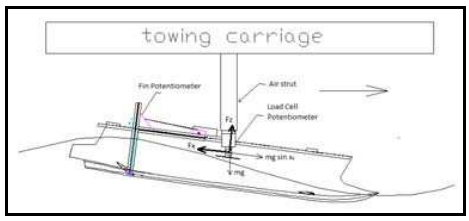

Figure **7** Seakeeping test using captive model.

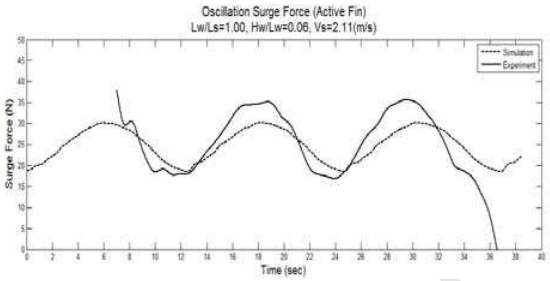

Figure 8 Validation of harmonic surge force in following sea

Lw/Ls=1.0; Hw/Lw=0.06 and Vm=2.m/s (Active Fin)

The decrease of the force indicates there is a weight force assisting the model to accelerate (surfing condition) or the increase of force measured indicates there is a weight force that causes the model to decelerate (climbing condition). Validation of the surge motion based on comparison the force is shown in Figure 8. The discrepancy might caused by the nonlinear effect of water flowing around the model particularly at the fin stabilizer.

Validation of vertical heave and pitch motion of simulation was conducted by comparing the heave displacement and pitch angle. The results of validation were shown in Figures 8-10. The solid line represents test results and dashed line represents simulation results. The validation results of heave showed the test has higher than simulation results, whilst the pitch angle and fin angle has a good comparison. The ripples signal of the heave and pitch model using active fin stabilizer maybe caused by the perturbation response of the fin stabilizer. The perturbation arise when the feedback signal of pitch angle and fin angle interrupted by noise.

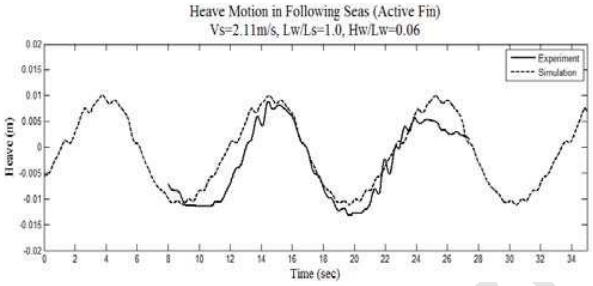

Figure 9 Validation of heave motion in following sea Lw/Ls=1; Hw/Lw=0.06 and Vm=2.11m/s (Active Fin)

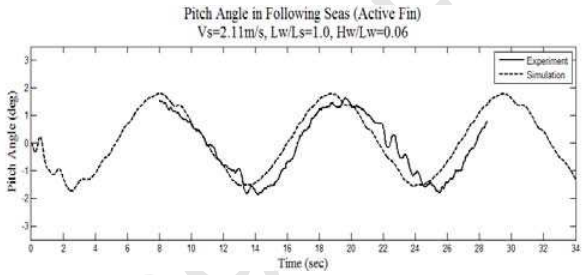

Figure 10 Validation of pitch motion in following sea Lw/Ls=1; Hw/Lw=0.06 and Vm=2.11m/s (Active Fin)

PARAMETRIC STUDY

Variations of parameters were initial ship speed ratio Vs/Vw in the range of 1.05-1.35, wavelength ratio Lw/Ls in the range of 1.0-2.0 and wave height ratio Hw/Lw was 0.07 and 0.08. The ship simulated with fixed and active fin stabilizer.

Figure 11, 12 and Figure 13, 14 showed the minimum clearance between foredeck and wave surface with fixed fin at bow and stern, and with fixed fin at bow and active fin at stern respectively. The ship was simulated iteratively to determine the initial speed ratio in which the clearance was minimum. The results present the submerged foredeck arise for steepness ratio 0.07, the ship with fixed fin at bow and stern, initial wavelength ratio between 1.05 and 1.4, initial ship speed ratio 1.26 and 1.33, whilst the ship with steepness ratio 0.08 arise at initial wavelength ratio up to 1.7, initial ship speed ratio between 1.24 and 1.33. The foredeck immersed at higher steepness ratio. The ship with fixed fin at bow and active fin stabilizer at stern is found the foredeck did not immerse, however the immersed foredeck tends arise with increase of steepness and wavelength at higher initial ratio ship speed.

Figure 15, 16 and Figure 17, 18 presented the range of speed change with fixed fin at bow and stern and with fixed fin at bow and active fin at stern respectively. The ship has a maximum speed when the ship is near the wave trough, a moment before the pitch angle turns to a positive direction. Minimum speed is near the wave crest, a moment

of speed changes was found decreased and tends to converge to a constant speed change with increase of initial speed. The mean speed found above the initial speed for the ship with all fixed fin stabilizer and it below the initial speed for the ship with active fin at stern. The range of speed changes for the ship with all fixed fin stabilizer is smaller than the ship with active fin at stern as shown in Figure 19 and Figure 20. It shows more surge of dynamic motion on the ship with fixed fin stabilizer. The mean of surge velocity tends has a constant change for all initial ship speed and increase with increase of wave steepness.

Figure 19 and Figure 20 showed the range of the ship speed change by the effect of surge motion from the minimum speed and the maximum speed. The range of the speed change compared between all fin stabilizer are fixed and with fixed fin at bow and active at stern.

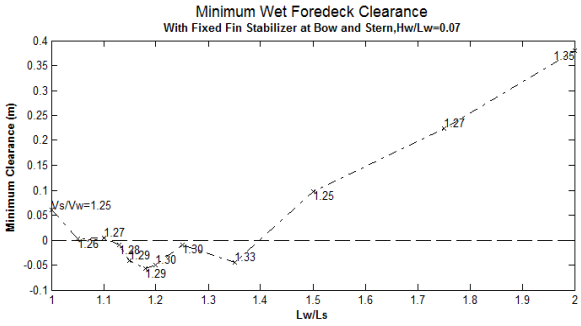

Figure 11 The initial Vs/Vw recorded at minimum foredeck clearance of time domain simulation, simulated at Hw/Lw=0.07 with a fixed fin stabilizer at bow and stern.

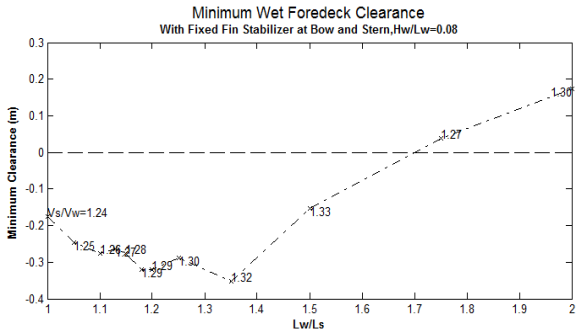

Figure 12 The initial Vs/Vw recorded at minimum wet foredeck clearance of time domain simulation, simulated at Hw/Lw=0.08 with a fixed fin stabilizer at bow and stern.

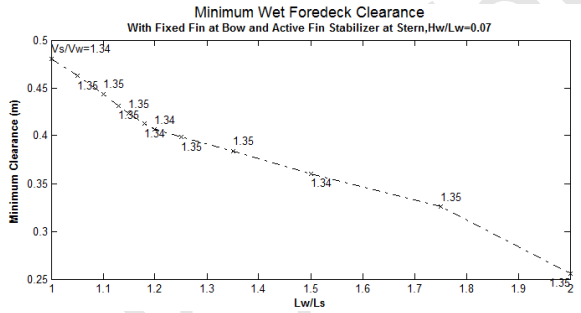

Figure 13 The initial Vs/Vw recorded at minimum wet foredeck clearance of time domain simulation, simulated at Hw/Lw=0.07 with a fixed fin stabilizer at bow and stern.

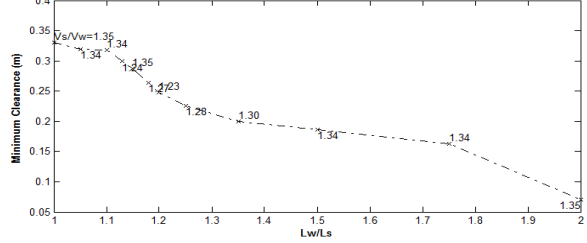

Figure 14 The minimum wet foredeck clearance recorded at certain Vs/Vw, was simulated at Hw/Lw=0.08. With fixed fin stabilizer at bow and active fin stabilizer at stern.

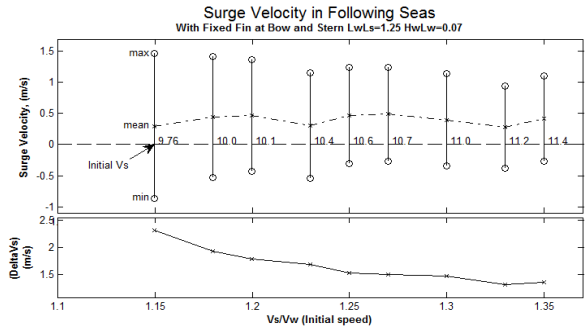

Figure 15 Minimum, maximum, mean of surge ship velocity in following seas (above). Delta of surge velocity (below) with fixed fin stabilizer at bow, and stern Lw/Ls=1.25 and Hw/Lw=0.07.

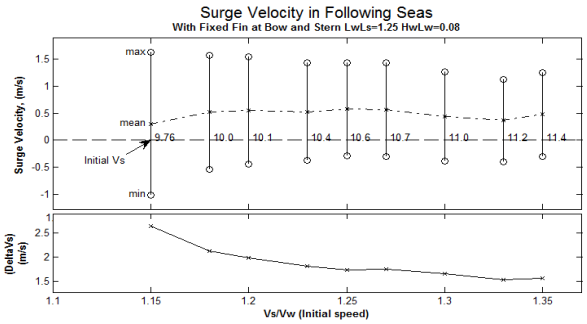

Figure 16: Minimum, maximum, mean of surge ship velocity in following seas (above). Delta of surge velocity (below) with fixed fin stabilizer at bow, and stern Lw/Ls=1.25 and Hw/Lw=0.08.

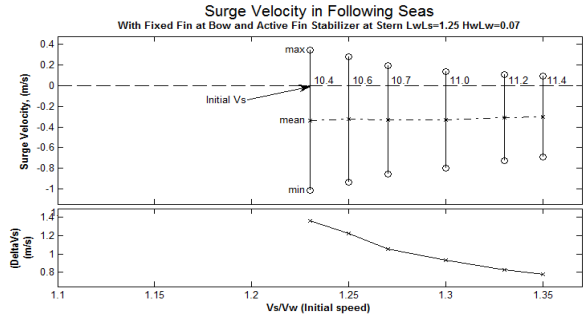

Figure 17: Minimum, maximum, mean of surge ship velocity in following seas (above). Delta of surge velocity (below) with fixed fin stabilizer at bow, and active fin at stern Lw/Ls=1.25 and Hw/Lw=0.07.

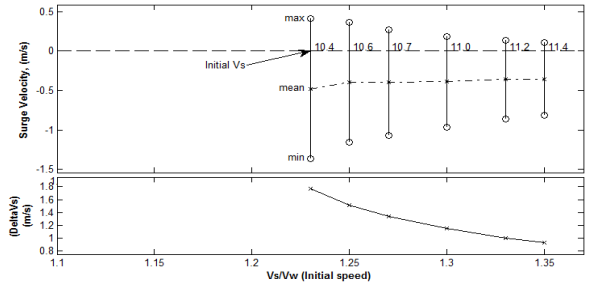

Figure 18: Minimum, maximum, mean of surge ship velocity in following seas (above). Delta of surge velocity (below) with fixed fin stabilizer at bow, and active fin at stern Lw/Ls=1.25 and Hw/Lw=0.08.

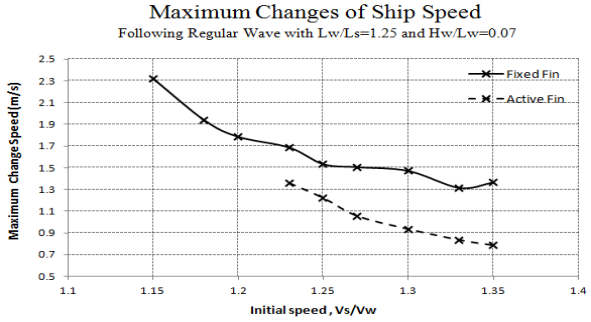

Figure 19: Maximum changes of ship speed from wave trough to wave crest for the ship running in following wave with Lw/Ls=1.25 and Hw/Lw=0.07.

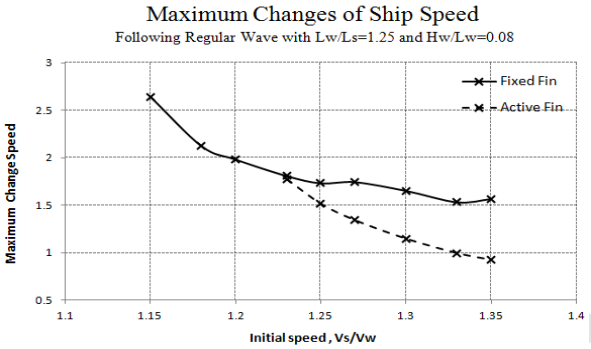

Figure 20: Maximum changes of ship speed from wave trough to wave crest for the ship running in following wave with Lw/Ls=1.25 and Hw/Lw=0.08.

SHIP MOTION ILLUSTRATION

Illustrations of the ship running in following sea with fixed and active fin stabilizer were shown in Figure 21and Figure 22. The response illustrates the critical condition of the ship running from the wave trough to the wave crest with active fin stabilizer at stern. It compared to the ship response using fixed fin at bow and at stern. In Figure 19 shows the ship running with fixed fin at bow and stern, simulated at Hw/Lw=0.08, Lw/Ls=2.0, and initial Vs/Vw=1.35 showed an immersed foredeck did not arise and the maximum angle at the wave crest was 8.64deg. The pitch angle showed a relative high because the fin stabilizer did not produce the force moments to battle the wave hull moment. In t=20 seconds, the ship running in acceleration from the wave crest to the wave trough showed the bow tends to the bow-dive condition. At t=21 seconds, the bow hull buoyancy began to reverse the pitch angle, and the speed is slow down, lifts the bow hull and then the ship having a positive pitch angle. The ship speed move to be backward relative to the wave profile.

In Figure 20, the ship illustrated running with fixed fin at the bow and active fin stabilizer at the stern. The ship was simulated at Hw/Lw=0.08, Lw/Ls=2.0, and initial Vs/Vw=1.35. The response showed the ship did not experience the immersed foredeck with maximum pitch angle during the ship at the wave crest was 5.18deg. The pitch angle compared to the illustration of the ship in Figure 19 has a lower angle by the effect of the fin stabilizer increase the force moment to battle the wave hull force and moment.

DISCUSSION

The ship experienced surfing and accelerating to the wave trough and decelerating to the wave crest for the change of maximum and minimum speed as shown in Figure 15 and Figure 16. The mean surge velocity is above the initial speed. It indicates the ship has a surfing condition that causes the ship with fixed fin at the bow and at the stern has a tendency to bow dive condition. The condition is arising at certain wavelength and at wave steepness. The ship surfing from the wave crest to the wave trough causes an increase of ship speed and then inertial force. The slender shape of the bow with a small waterplane area is also has a low restoring force so it cannot restrain the longitudinal inertial force. It causes a tendency of the bow dive condition even the immersed foredeck is increased. Moreover, in surfing, the vertical damping force of fixed fin is dominant, greater than the buoyancy force when in the high speed. It influences the bow dive condition is sustained. At the same time, the buoyancy force will increase when the submergence of the bow is increased, then ship speed begins to slow down, and the resultant forces to lift the bow become dominant cause the pitch angle turns to a positive direction as shown in Figure 21 and Figure 22.

The ship using the active fin stabilizer can prevent the ship from the bow-dive condition as shown in Figure 17 and Figure 18. The fin reduces the tendency of bow dive by the increase of the fin stabilizer moment, decrease pitch angle and then the surge velocity will decrease, shown by the mean speed is below the initial speed. It indicates the fin restrains the ship from surfing condition. From the response of surge motion, it showed the initial speed ratio has a significant effect to the surge velocity change. It is because the active fin stabilizer can regulate the fin angle according to the feedback variable of pitch angle. Comparing the range in change of surge velocity, the ship with fixed fin at bow and active fin stabilizer at stern showed the effectiveness of an active fin stabilizer restrain the ship from surfing condition as shown in Figure 19 and Figure 20. The range of speed change decrease with increase of initial speed ratio for fixed fin or active fin but the discrepancy between the ranges is increase. It shows that the ship speed has significant effect of the fin to increase the damping as well as the moment stabilizer. The fin also showed reducing the pitch angle up to 40%, comparing the pitch angle in Figure 21 and Figure 22.

The seakeeping performance with fixed and active fin stabilizer running in long wavelength and high ship speed was presented in illustration of the ship surfing to the wave trough as shown in Figure 21 and Figure 22. The ship with fixed fin experience a high pitch angle and the bow buoyancy raise the bow hull let the ship did not meet the immersed bow condition, whilst the ship with active fin has low pitch angle, and the foredeck tends to be immersed. This illustration presents the conditions as described in Figure 11 up to Figure 14.

CONCLUSION

Based on the results of parametric simulation and illustration of the ship in wave can be drawn as follows;

The ship using fixed fin stabilizer at bow and at stern has a possibility of the bow-dive arise is higher than active fin, even resulted in the

tends have an immersed foredeck with increase of wavelength and initial ship speed.

The ship with active fin stabilizer reduces the surfing condition significantly and prevents the ship to have a bow-dive condition. However, the condition cannot be ignored when the wave steepness or initial ship speed increase significantly.

The mean of speed change in harmonic motion has tendency to be constant linear to the wave steepness and has no significant effect to wavelength ratio change found for all fixed fin stabilizer and active fin stabilizer at stern.

ACKNOWLEDGMENT

This research successfully conducted with the support of various parties. Thanks to the ministry of education of Malaysia, MOSTI in supporting this research, as well as the ministry of education of Indonesia, the government of Sulawesi Selatan Indonesia for all support in this research. In addition, thanks to Zakaria, Ismail, Azlan, Radzief, Syahrizan, Ali for all supports in testing in towing tank.

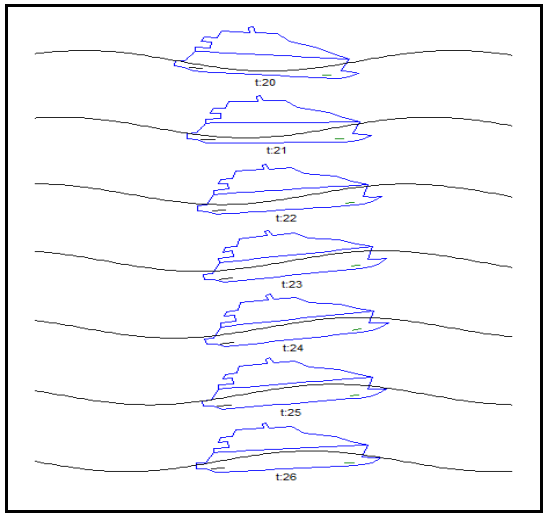

Figure 21 Simulation ship with fixed fin at bow and stern, Lw/Ls=2.0, Hw/Lw=0.08 and Vs/Vw=1.35. Maximum pitch angle at wave crest was 8.64 deg.

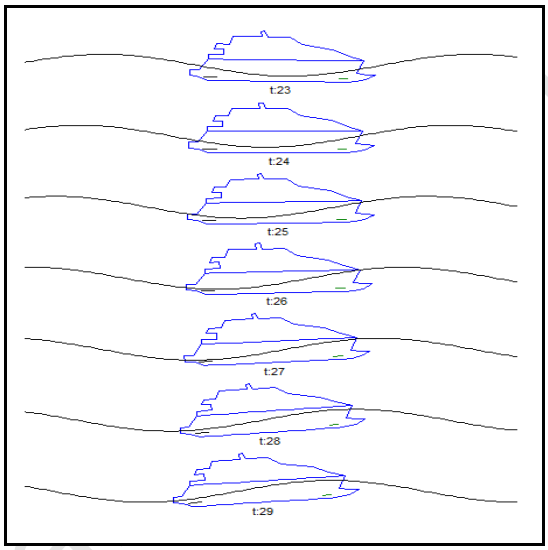

Lw/Ls=2.0, Hw/Lw=0.08 and Vs/Vw=1.35. The pitch angle at wave crest 5.18 deg. Foredeck did not immersed.

REFERENCES

Amerongen, J. V. (1982). Adaptive Steering of Ships-A Model Reference Approach to Improved Maneouvering and Economic Course. PhD, Delf University, Netherland.

Bhattacharya, R. (1978). Dynamics of Marine Vehicles. New York: John Wiley & Sons.

Brien, J. T. O., & Kuchenreuther, D. I. (1957). Free Oscillation in Surge and Sway of A Moored Floating Dr Dock. Paper presented at the 6th ICCE, Gainesville, Florida.

Chin, N., Roberts, G., Scrace, R., & Owens, D. (1994). Mathematical Model of A Small Water Plane Area Twin Hull (SWATH) Vessel. Paper presented at the Control International Conference

Dand, I. W. (2006, 31 Oct - 1 Nov 2006). High Speed Craft Bow Diving in Following Seas. Paper presented at the ACV's, WIG's and Hydrofoil, London, UK.

Djackov, V. (2005). The Research of Pitching and Heaving Stabilization of Fast Catamaran PhD, Klaipeda University, Kaunas,.

Faltinsen, O. M. (2005). Hydrodynamics of High-Speed Marine Vehicles: Cambridge University press.

Fang, C. C., & Chan, H. S. (2004). Investigation of Seakeeping Characteristics of High Speed Catamaran in waves. Journal of Marine Science and Technology, 12, pp.7-15.

Folso, R. (2004). Comfort Monitoring of high-speed passenger ferries. PhD, Technical University of denmark.

Kan, M. (1990). Surging of Large Amplitude and Surf-Riding of Ships in Following Seas Naval Architecture and Ocean Engineering (1990 ed., Vol. 28). Tokyo: The Society of Naval Architecture of Japan, .

Kenevissi, F., Atlar, M., & Mesbahi, E. (2003). A New Generation Motion Control System for Twin-Hull Vessels Using a Neural Optimal Controller. Marine Technology and SNAME News 40(3), pp.168-180.

Kim, Y.-H. (1992). Trust Deduction Prediction For High Speed Combathan Ship. Bethesda Maryland: David Taylor Research Centre.

Klught, P. G. M. V. D. (1987). Rudder Roll Stabilization. PhD, Delf University of Technology, Nederland.

Lloyd, A. R. J. M. (1998). Seakeeping: Ship Behavior In Rough Weather (1 ed. Vol. 1): Ellis Horwood.

Maimun, A. (1993). Stability of Fishing Vessels in Astern Sea Shallow Water Environment. PhD, Strathclyde University, Glasgow.

Matsuda, A., Hasimoto, H., & Umeda, N. (2004). Capsizing Due to Bow-Diving in Following Waves. International Ship building, 51, 13.

Papanikolaou, A., & Soares, C. G. (2009). Risk-Based Ship Design: Methods, Tools and Applications. Berlin: Springer.

Perez, T. (2005). Ship Motion Control (1 ed.). Norway: Springer.

Spyrou, K. J. (2006). Asymetric Surging of Ships in Following Seas and Its Repercussions for Safety. NonLinear dynamics, 43, pp.149-172.

Spyrou, K. J., & Tingkas, I. G. (2011). Nonlinear surge dynamics of a ship in astern seas: Continuation analysis of a periodic states with hydrodynamic memory. Journal of Ship Research, 55(1), pp.19-28.

Stevens, S. C., & Parsons, M. G. (2002). Effects of Motion at Sea on Crew Performance: a Survey. Marine Technology and SANME News, 39, pp.29-47.

Umeda, N. (1990). Probabilistic Study on Surf-Riding of a Ship in Irregular Following Seas. Paper presented at the STAB 90, Stability of Ships & Ocean Vehicles, Naples, Italia.

Whicker, L. F., & Fehlner, L. F. (1958). Free-Stream Characteristics of A Family of Low Aspect Ratio All Movable Control Surfaces For Application to Ship Design (Hydromechanics, Trans.): David Taylor Model Basin.

Wu, W., Spyrou, K. J., & McCue, L. S. (2010). Improved Prediction of the Treshold of Surf-Riding of A Ship in Steep Following Sea. Ocean Engineering, 37, pp.1103-1110.